J. Electrochem. Sci. Eng. **13(2)** (2023) 347-360; http://dx.doi.org/10.5599/jese.1501

Open Access : : ISSN 1847-9286
www.jESE-online.org

Original scientific paper

Hybrid polymer inclusion membrane as anion exchange membrane for recovering Pd^{2+} ions in electrogenerative process

Syed Fariq Fathullah Syed Yaacob✉, Nadia Mansor, Syaza Atikah Nizar, Ayo Olasupo, Norita Mohamed and Faiz Bukhari Mohd Suah✉

Green Analytical Chemistry Laboratory, School of Chemical Sciences, Universiti Sains Malaysia, 11800 Minden, Pulau Pinang, Malaysia

Corresponding authors: ✉syedfariq@usm.my; ✉fsuah@usm.my

Received: August 23, 2022; Accepted: November 23, 2022; Published: December 8, 2022

Abstract

A novel non-plasticized nano-porous hybrid inorganic-organic polymer inclusion membrane (PIM) was synthesized, characterized, and evaluated as an anion exchange membrane for application in electrogenerative processes to recover Pd^{2+} ions. Ionic liquids 1-ethyl-3-methylimidazolium chloride (EMIM-Cl) and 1-butyl-3-methylimidazolium chloride (BMIM-Cl) were used as the carrier molecules in the polymeric network of PIM to enhance anion exchange process. This hybrid anion exchange membrane also consists of a polymeric matrix of non-plasticized cellulose triacetate modified by incorporating an inorganic material (silane) prepared by the sol-gel route. Different parameters affecting the ion transport performance efficiency, i.e., the composition of the membrane, type of ionic liquid (carrier molecule) and ion–exchange capacity, were investigated and optimized. In the electrogenerative process, the results revealed that the prepared PIM yields better recovery results for recovering Pd^{2+} ions from its chloride solution compared to the commercial anion exchange membrane Neosepta® AM-01, with a full recovery of 100 mg/L Pd^{2+} ions in 30 min. This preliminary study shows that the prepared low-cost hybrid anion exchange membrane PIM can act as an inexpensive material suitable for the rapid and efficient recovery of Pd^{2+} ions from an aqueous solution.

Keywords

Hybrid inorganic-organic membrane; chloride solution; ionic liquids

Introduction

An electrogenerative process is a spontaneous electrochemical process that reduces (more noble) metal ions to elemental metal at the cathode [1]. As in a galvanic system, the energy associated with chemical reactions is converted into electrical energy or direct current electricity as a by-product. Although electrogenerative systems and fuel systems use catalytic electrodes, the cell components differ in their primary function [2]. The emphasis on chemical processing in electro-

generative processes results in special considerations for these types of systems, such as product recovery [3]. In general, the setup for an electrogenerative process consists of two electrodes (cathode and anode), electrolytes (catholyte and anolyte), an ion exchange membrane, and an external cable to complete the circuit [4].

The electrogenerative process is driven by an oxidation-reduction reaction. The anode side is where oxidation occurs with the substance losing electrons, while reduction occurs on the cathode side, which gains electrons (*e.g.*, the oxidant Pd^{2+} gains electrons to become Pd^0). The standard reduction potential for the half-cell reaction shows an overall positive cell potential, resulting in the spontaneous deposition of the reduced metal (Pd^0) onto the cathode. The effect of Pd deposition on the membrane was further investigated.

Anode: $Zn^{2+} + 2e^- \rightleftharpoons Zn$ $E°_{ox} = -0.763$ V *vs.* SHE (1)

Cathode: $Pd^{2+} + 2e^- \rightleftharpoons Pd$ $E°_{red} = +0.981$ V *vs.* SHE (2)

Overall: $Zn + Pd^{2+} \rightleftharpoons Zn^{2+} + Pd$ $E°_{cell} = +1.744$ V vs. SHE (3)

Ion exchange membranes are semi-permeable membranes composed of ionic head groups attached to polymer matrices [5]. Depending on the type of ion permitted to cross the membrane layer, they can be classified as anion exchange membranes, cation exchange membranes or bipolar membranes [6,7]. For example, anion exchange membranes contain positively charged head groups in the membrane, which permit the passage of anions while repelling cations [6]. By exploiting the selective nature of ion exchange membranes, anion and cation exchange membranes can be adapted for various applications. Commercially available ion exchange membranes are primarily found in water treatment applications such as desalination or high-purity water production in food and beverage, as well as in pharmaceuticals, semiconductors, power generation, fuel cells, electrodialysis, Donnan analysis, electrolysis and many more [4-15].

One type of ion exchange membrane is a hybrid inorganic-organic ion exchange membrane. Inorganic–organic composite materials are increasingly important due to their extraordinary properties within a single molecular composite, which arise from the synergism between the individual component properties [16]. A sol-gel method can be used to prepare this hybrid membrane by adding a silane into the organic membrane. The purpose of adding silane to the membrane is to provide beneficial impacts to the organic polymeric membrane (cellulose triacetate). In particular, adding silane will assist the migration of ions across the anion-exchange membrane, resulting in better mass transport due to the formation of hydrated microchannels. These materials have gained much interest due to the transformation in their properties, such as mechanical, thermal, electrical, and magnetic properties, compared to pure organic polymers or inorganic materials [17-20]. In these composites, organic materials offer structural flexibility, convenient processing, tunable electronic properties, photoconductivity, efficient luminescence, and the potential for semiconducting and metallic behaviour. Inorganic compounds provide the potential for high carrier mobilities, bandgap tunability, a range of magnetic and dielectric properties, and thermal and mechanical stability. In addition to combining distinct characteristics, new or enhanced phenomena can also arise due to the interface formed between the organic and inorganic components [21,22].

To date, only commercially available anion exchange membranes, namely Neosepta® AM-01 and Neosepta® AMX, have been utilized in an electrogenerative process [23,24]. However, the commercially available anion exchange membranes are costly, produced for general (non-specific) applications, and have low dimensional ability and high solute diffusion rates. Using polymer inclusion membranes (PIMs) as anion exchange membranes in electrogenerative processes was already proposed with remarkable results [25]. To further improve the performance of PIMs, a non-

plasticized nano-porous hybrid inorganic-organic anion exchange PIM containing an ionic liquid has been introduced in this study. This study aims to prepare and characterize the novel nano-porous hybrid inorganic-organic anion exchange PIM and evaluate its performance as an anion exchange membrane in the electrogenerative process for recovering Pd^{2+} ions from a chloride solution.

Experimental

Chemicals and materials

For hybrid PIM preparation, tetraethyl orthosilicate (TEOS) and dichlorodimethylsilane (DCDMS) from Sigma Aldrich, UK, were used to obtain the silane mixture. Trioctylmethylammonium chloride (Aliquat 336), 1-ethyl-3-methylimidazolium chloride (EMIM-Cl) and 1-butyl-3-methylimidazolium chloride (BMIM-Cl) from Sigma Aldrich (United Kingdom) were used as a carrier in the membrane, and cellulose triacetate (CTA) (Acros, Malaysia) was used as organic support to provide the polymeric mechanical strength. The commercial anion exchange membrane was Neosepta AM-01 (Tokuyama Corp., Japan). Chemicals such as palladium(II) chloride, chloroform and diethyl ether were obtained from QReC Chemicals. The electrogenerative batch cell design was the same as in our previous work [1], with each compartment 5.0×4.5×6.5 cm. The cathode used in this experiment was reticulated vitreous carbon (RVC) (The Electrosynthesis Co., USA) with dimensions 2.5×1.0×0.6 cm, pre-treated with concentrated H_2SO_4. Zinc foil (99 % purity) (2.5×1.0×0.05 cm) was used as the anode and polished with sandpaper before rinsing with distilled water and ethanol. The membrane was cut into dimensions that fit the cell and filled with water before use. All experiments were run for 4 h at room temperature.

Silane mixture preparation

A multistage procedure prepared the inorganic part of the membrane consisting of a silane mixture. 4 mL of dichlorodimethylsilane (DCDMS) was dissolved in 10 mL of diethyl ether, and then 1.5 mL of water was added in aliquots of 0.5 mL every 20 min and mixed for 1 h in an iced water bath. Later, both immiscible phases were separated, and 1 mL of tetraethylorthosilicate (TEOS) was added to the extracted organic phase to obtain a cross-linked network. Finally, the homogenous sol-gel mixture was kept in the water bath for 5 days at 50 °C.

Hybrid PIM membrane preparation

For membrane samples preparation, the organic part of the membrane was prepared by dissolving different amounts of cellulose triacetate (CTA) and carrier in chloroform. The obtained silane mixture (0.03 g) was added to the organic solution, and all components were vigorously stirred to mix them homogeneously. The resulting solution was poured into a Petri dish and allowed to evaporate for over 24 h at room temperature. The polymer inclusion membrane (PIM) was later cured in an oven at 80 °C for 20 h and stored in a sealed bag. The process is shown in Figure 1.

Hybrid membrane characterization

The thickness of the membrane and its surface morphology were measured with an electronic digital micrometer and corroborated with Scanning electron microscopy (SEM) (Quanta 650, USA). The membrane functional groups were identified using Fourier transform infrared (FT-IR) spectrometer (Perkin Elmer Model System 2000, USA). Measurement was scanned in the frequency range of 400 to 4000 cm^{-1} and analysed using commercial software.

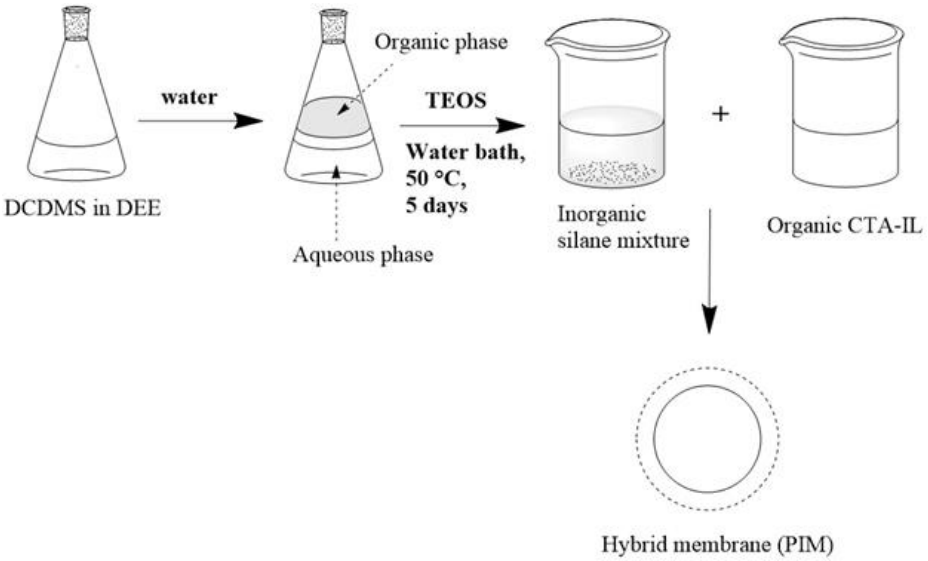

Figure 1. *Schematized procedure for preparation of nano-porous hybrid inorganic-organic anion exchange PIM (DCDMS: dichlorodimethylsilane, DEE: diethyl ether, TEOS: tetraethoxysilane, CTA: cellulose triacetate, IL: ionic liquid)*

Electrogenerative experiment

The optimum condition of Pd^{2+} ions recovery was studied using a batch cell, similar to what was reported by Mansor *et al*. [23]. The batch cell configuration was used for each experiment at room temperature (Figure 2). During the electrogenerative experiment, electrodes with attached copper collectors were linked to a multimeter to measure the potential of electrodes, as well as the flow of electric current. In order to compare the differences in the concentration of Pd^{2+} left in the solution after being deposited on the cathode, 500 µL of the catholyte solution was initially removed, and this procedure was repeated frequently every 30 minutes during the tests. At the same time, every withdrawn aliquot was substituted with 500 µL of distilled water to ensure the same volume of both electrolytes. Prior to analysis, the aliquot samples were diluted with distilled water to a volume of 25 mL in 60 mL plastic bottles.

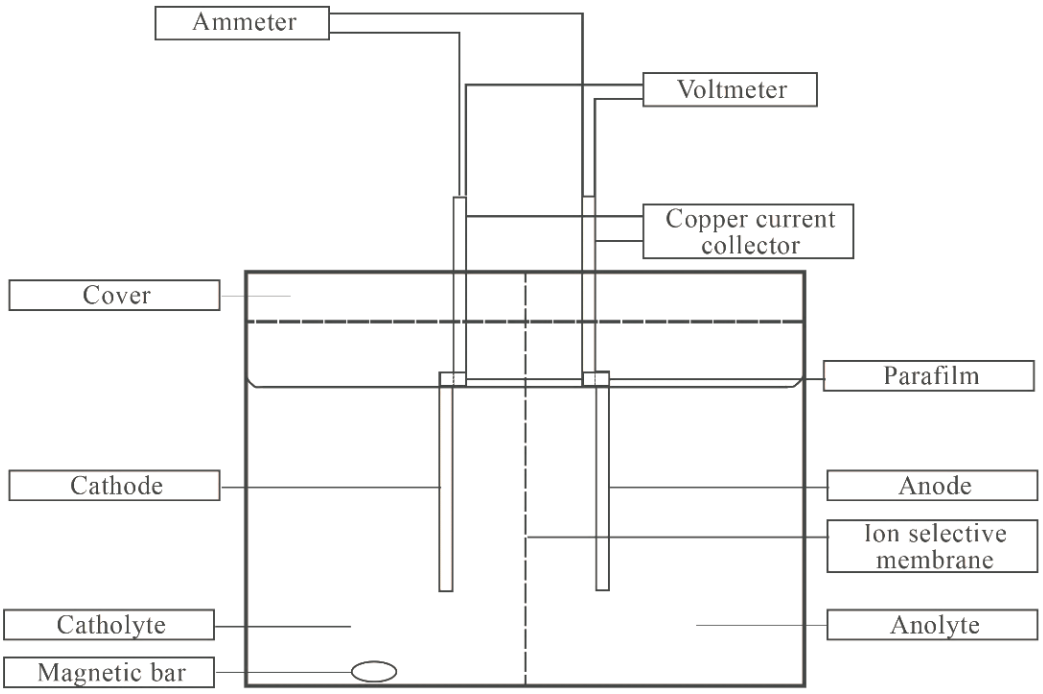

Figure 2. *Experimental setup of the batch cell*

Atomic absorption spectroscopy, AAS (Perkin Elmer Analyst 200 Model, USA) with a wavelength of 247.6 nm was then used to analyze Pd^{2+} recovery concentrations every 30 minutes over the 6-hour experiment. A blank and various Pd^{2+} standard solutions at concentrations of 1, 2, 3, 4, 5, and 10 mg L^{-1} were examined for calibration curve analysis.

The calculation of the recovery in % is presented in equation (4).

$$\text{Pd recovery} = \frac{C_0 - C_t}{C_0} 100 \quad (4)$$

where C_o is the initial and C_t is the Pd concentration, mg L^{-1}, at time t.

Polarization of the membrane

A voltmeter measured the potential of the RVC cathode against the reference electrode (saturated calomel electrode, SCE) (Hanna Instruments, Malaysia). Initially, the cell was connected to a resistance box loaded with a maximum resistance of 9.99 MΩ and was decreased gradually until the minimum of 1 Ω. The system was allowed to reach a steady state for 3 min after each change in the resistance value. Later, the cathode potential and current readings were recorded, and the cathodic polarization curves were plotted.

Results and discussion

Membrane characterization

Membrane composition

For the preliminary studies using different types of ILs (Figure 3), the PIM composition was prepared by mixing 0.10 g of CTA and 0.08 g of IL, followed by 0.03 g of silane.

It is shown in Table 1 that among three tested hybrid membranes (PIM1-PIM3), the excellent recovery of Pd^{2+} ions (100 mg/L) is obtained in the presence of BMIM-Cl (PIM2). The presence of extra Cl^- ions in the hybrid membrane enhances the mass transfer process, which subsequently increases the recovery of Pd^{2+} ions [26]. Further studies were conducted using different quantities of BMIM-Cl due to its direct relationship with transport efficiency and results are shown in Table 2.

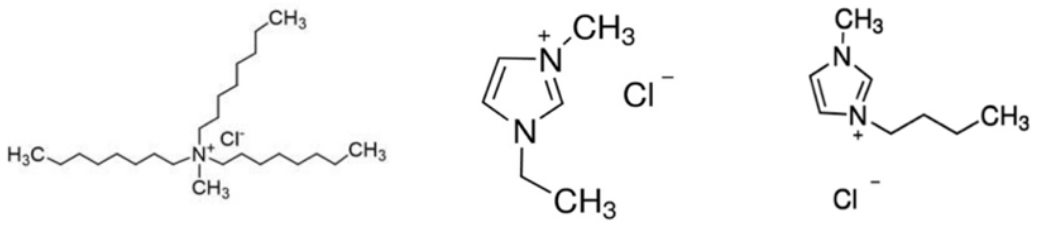

Figure 3. *Different types of ionic liquids (ILs) used in this study*

Table 1. *Hybrid PIM compositions*

Membrane	Mass, g			Content, wt.%	Recovery, %
	CTA	IL	Silanes		
Blank	0.1	-	-	-	-
PIM 1: IL (Aliquat 336)	0.1	0.08	0.03	48:38:14	84.0
PIM 2: IL (BMIM-Cl)	0.1	0.08	0.03	48:38:14	99.9
PIM 3: IL (EMIM-Cl)	0.1	0.08	0.03	48:38:14	93.0

Table 2. *Optimization of BMIM-Cl concentration for hybrid PIM*

Membrane	Mass, g			Content, wt.%
	CTA	BMIM-Cl	Silanes	
Blank	0.10	-	-	-
I	0.10	0.08	0.03	48:38:14
II	0.14	0.14	0.03	37:52:11
III	0.12	0.12	0.03	44.5:44.5:11
IV	0.12	0.12	0.05	41.5:41.5:17

It was observed that when the excess transporting agent was added (> 0.10 g), a sticky and fragile membrane unsuitable for transport was formed. Similarly, adding too much silane (> 0.05 g) resulted in a crusty membrane surface and a non-homogeneous film. In addition, experimental results showed that it is necessary to cover the Petri dish with filter paper to slow the evaporation of the solvent and promote even drying, producing a clear, transparent, and homogeneous film.

Identification of membrane spectroscopic composition

In this study, ATR-FTIR analysis was performed to confirm the presence of the main components of the PIM membrane by identifying the most important peaks (Figure 4 and Table 3).

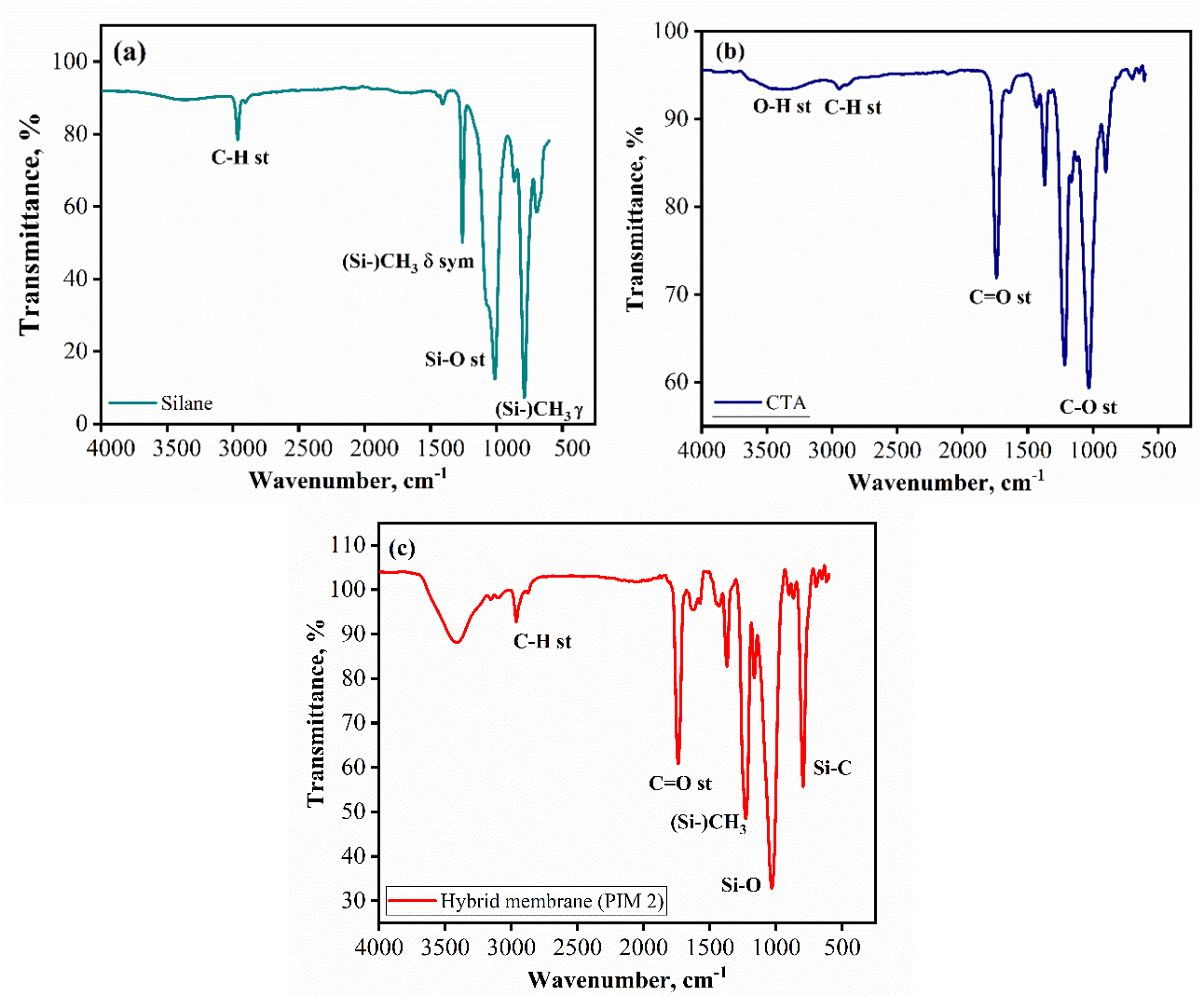

Figure 4. *ATR-FTIR spectra of different isolated components of hybrid membrane: (a) silanes, (b) cellulose triacetate (CTA) and (c) hybrid membrane (PIM 2)*

***Table 3**: Values of wavenumbers and types of molecular vibrations for each constituent material and hybrid membrane*

Materials	Wavenumber, cm^{-1}	Type of molecular structure
CTA	3365–3079	O – H
	2944	C – H
	1721	C = O stretching
	1203 - 1025	C – O – C
Silanes	1258	(Si –)CH_3
	1021	Si – O
	801	Si – C
PIM 2	3230–3578	Quarternary amine
	2969	C – H
	1751	C = O
	1258	(Si –)CH_3
	1021	Si – O
	801	Si – C

As shown in Figure 4(a), the ATR-FTIR spectrum of the silane mixture shows an absorption band at 801 cm^{-1} corresponding to the Si–C stretching in $Si(CH_3)_2$. The absorption bands observed at 1258 cm^{-1} and 1021 cm^{-1} correspond to the symmetrical deformation vibration of (Si–)CH_3 and Si–O stretching, respectively. Figure 4(b) shows that the absorption band located around 1721 cm^{-1} corresponds to stretching vibrations of the carbonyl group of CTA. The firm peaks at 1203 and 1025 cm^{-1} reflect the stretching modes of C–O–C symmetric and asymmetric bonds of CTA. Meanwhile, less intense bands seen at 2944 cm^{-1} are attributed to C–H bonds, and the absorption for O–H bonds stretching modes are observed in the region of 3365–3079 cm^{-1}. Figure 4(c) shows the expected bands related to the primary products described above: Si–C, (Si–)CH_3, and Si–O peaks from silane mixtures, and the C=O stretching vibration at 1751 cm^{-1} due to the presence of CTA. The peak at 2969 cm^{-1} is the aliphatic asymmetric and symmetric (C–H) stretching vibration due to the methyl groups in BMIM-Cl. A broad peak in 3230–3578 cm^{-1} corresponds to quaternary amine salt formation with chlorine. Based on the membrane spectrum, there are no signs of covalent bond formation between CTA, BMIM-Cl and silane. This implies only weak interactions between membrane components, such as hydrophobic, Van der Waals and/or hydrogen bonds.

Morphological properties of PIMs

Figure 5 shows SEM images of all prepared PIMs, *i.e.,* CTA, CTA–Aliquat 336–Silane, CTA–BMIM-Cl–Silane, and CTA–EMIM-Cl–Silane. These images are presented as cross-sections (i) and surface sections (ii).

As shown in Figure 5a, the surface of the CTA membrane appears dense and non-porous, whereas the PIM membranes shown in Figures 5b to 5d possess a porous structure.

The membrane cross sections in Figures 5b and 5c show estimated membrane thicknesses of 20 to 30 µM, which is very suitable for mass transport. This is because as the membrane thickness increases, the metal ion transport decreases due to the membrane resistance [27]. Higher porosity, with larger pores than the others, are observed for the membrane containing ionic liquid BMIM-Cl (PIM 2) (Figures 5c and 5e). This suggests that the larger pore size may increase the rate of ion movement across the membrane.

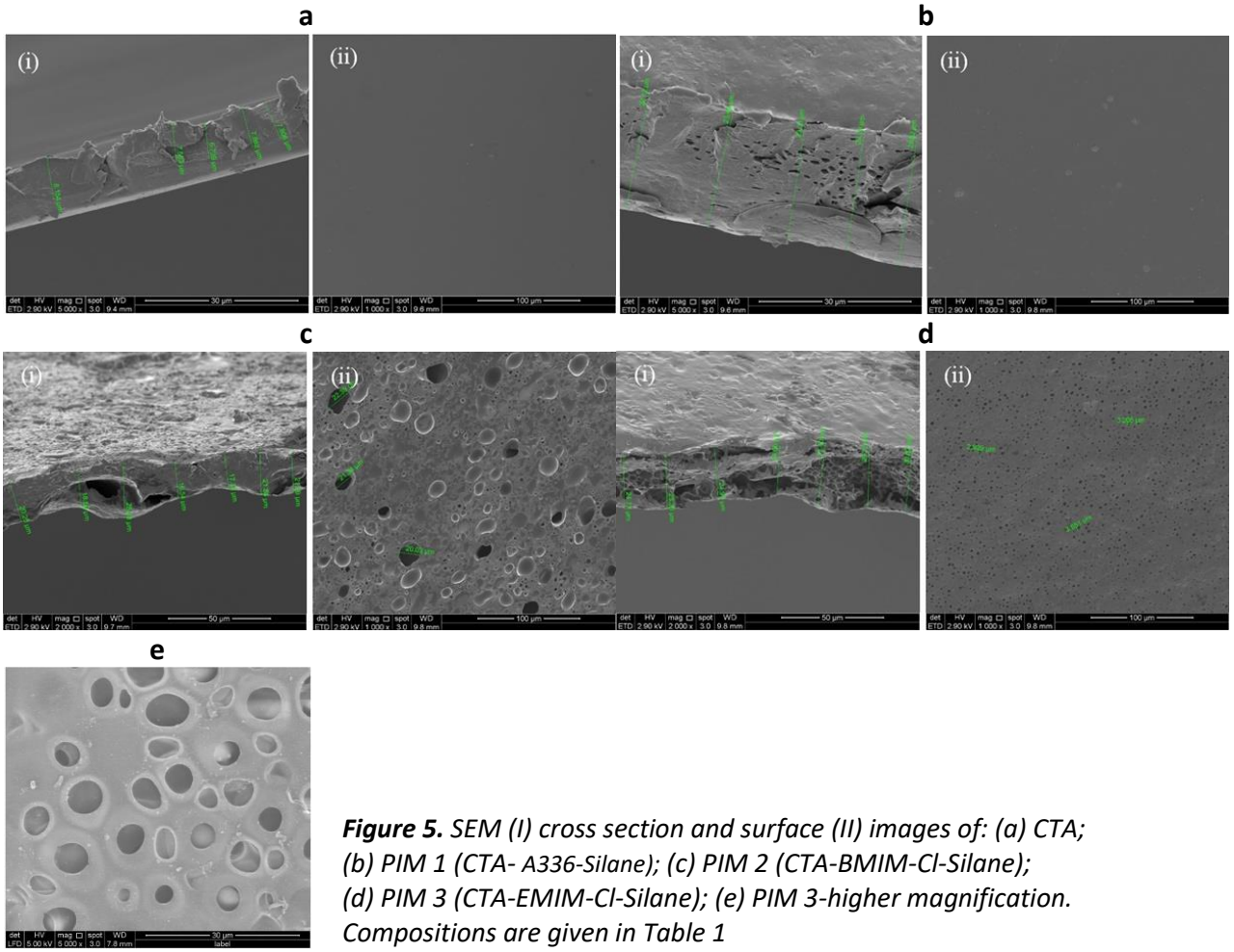

Figure 5. *SEM (I) cross section and surface (II) images of: (a) CTA; (b) PIM 1 (CTA- A336-Silane); (c) PIM 2 (CTA-BMIM-Cl-Silane); (d) PIM 3 (CTA-EMIM-Cl-Silane); (e) PIM 3-higher magnification. Compositions are given in Table 1*

Optimization of Pd^{2+} ions recovery process

Effect of different types of ILs

The efficiency of different ILs for the recovery of Pd^{2+} ions is illustrated in Figure 6.

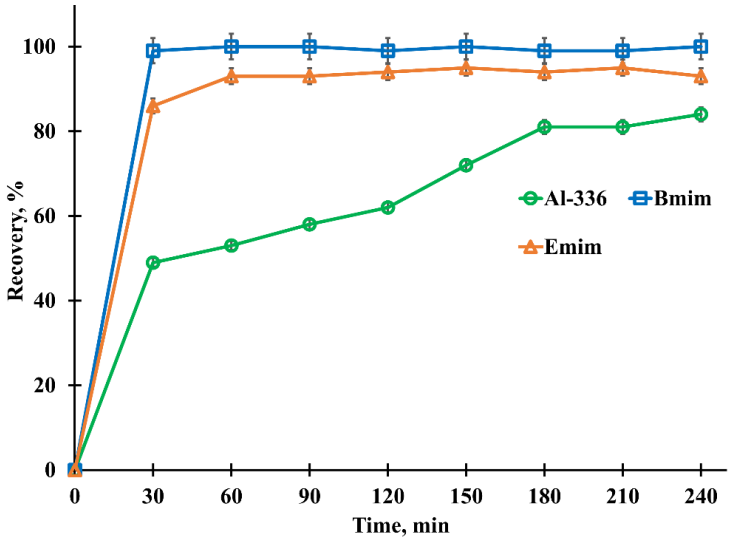

Figure 6. *Percent of recovery of 100 mg/L Pd^{2+} in 0.2.M NaCl vs. time with different types of ionic liquids used in PIMs*

As shown in Table 1, using BMIM-Cl as the ion-exchanger (carrier) in the hybrid PIM resulted in the highest recovery of Pd^{2+} ions with 99.9 % recovery, followed by EMIM-Cl with 93.0 %, and Aliquat

336 (84.0%). The efficiency of these ILs as ion exchangers depends on numerous factors, including the anolyte pH, the catholyte concentration, the amount of carrier used, the type of contaminants, membrane morphology, the molecular weight of the carrier, and others [23,24]. However, for comparison, the investigation was conducted under identical experimental conditions. The lower recovery of Pd^{2+} ions when Aliquat 336 was used could be attributed to the surface morphology of the Aliquat 336-based membrane and the molecular weight of the carrier. According to the SEM image in Figure 5b, the Aliquat 336-based membrane shows a smooth surface with no apparent porosity compared to BMIM-Cl, which has a large pore size (Figures 5b and 5e). Furthermore, the molecular weight of Aliquat 336 is higher than that of BMIM-Cl and EMIM-Cl. Thus, due to the lack of porosity, it might be difficult for the carrier to permeate the interface of the PIM during ion exchange with the anionic moiety of the anolyte. Hence, subsequent experiments were conducted using BMIM-Cl as the IL of choice.

Effect of different PIM compositions

The fastest recovery of Pd^{2+} ions was achieved using a PIM with a composition of CTA 0.1 g, BMIM-Cl 0.08 g, silane 0.03 g, where 99.9 % recovery was achieved in 30 min (Figure 7). From visual observation, this PIM composition formed a transparent film, which was smoother and more homogeneous than other PIMs (Table 4). It has been reported that high silane concentrations can affect the membrane appearance, resulting in a crusty layer and non-homogeneous characteristics [27]. A similar result was observed for the PIM with a composition of CTA 0.12 g, BMIM-Cl 0.12 g, and silane 0.05 g. Hence, the PIM composition CTA 0.1 g: BMIM-Cl 0.08 g: silane 0.03 g is preferred and chosen for additional analysis.

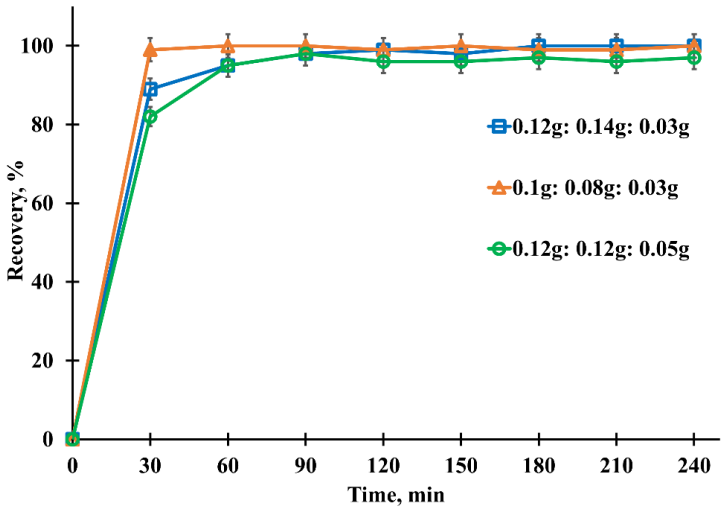

***Figure 7**. Percent of recovery of 100 mg/L Pd^{2+} in 0.2.M NaCl vs. time for different compositions of PIM (CTA-BMIM-Cl silane)*

***Table 4.** Pd recovery and visual observation of different compositions in CTA-BMIM-silane membrane*

Mass, g (CTA : BMIM : silane)	0.10 : 0.08 : 0.03	0.12 : 0.14 : 0.03	0.12 : 0.12 : 0.05	0.20 : 0.00 : 0.03
Time (99.9 %), min	30	120	Analysis not conducted	>30
Visual		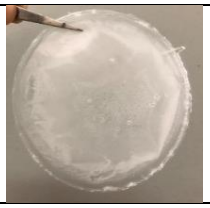	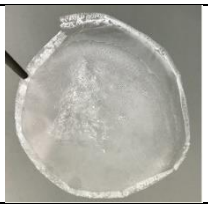	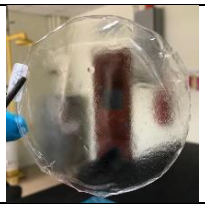

Effect of silane in PIM composition

Figure 8 shows the effect of silane presence on the recovery of Pd^{2+} ion. It can be seen that the introduction of silane into the membrane matrix slightly increases the Pd^{2+} ion recovery rate. Complete recovery of Pd^{2+} ions was achieved after 30 min using hybrid PIMs containing silane. The presence of silane in the PIM matrix could enhance the migration of ions and resulting mass transport due to the formation of hydrated microchannels and higher porosity [25,28]. Therefore, the hybrid PIM containing silane was selected for this study.

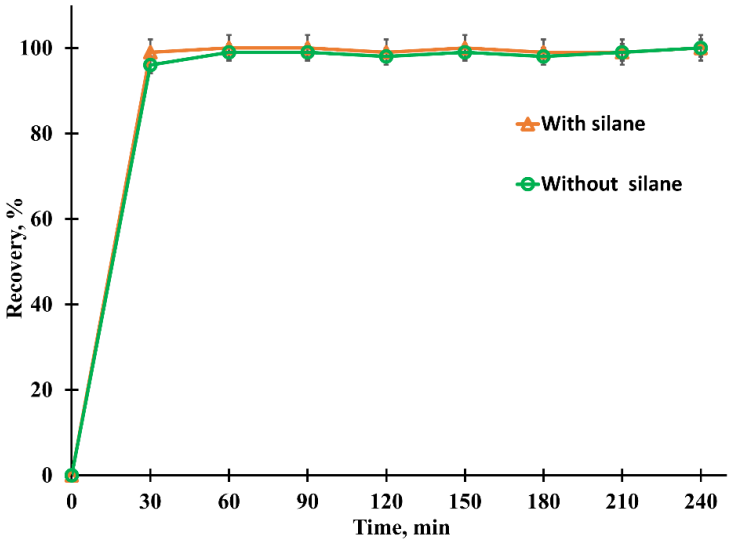

Figure 8. *Effect of silane in PIM on recovery of 100 mg/L of Pd^{2+} in 0.2 M NaCl. PIM composition: 0.1 g CTA, 0.08 g BMIM-Cl, 0.03 g silane*

Effect of different types of membranes

Three different types of membranes were utilized in this electrogenerative study, *i.e.,* PIM consisting of 0.1 g CTA, 0.08 g BMIM-Cl, 0.03 g silane, Neosepta AM-01 anion exchange membrane and pure CTA membrane. The initial study showed the cell voltage generated during full recovery of Pd^{2+} ions (after 30 min of the experiment) using different membranes as the anion exchange membrane was 510.20 mV for PIM, 495.3 mV for Neosepta AM-01 membrane, and 30.6 mV for CTA membrane. A high voltage potential value indicates a high deposition of Pd^{2+} ions onto the cathode [25]. This manifests that the presence of BMIM-Cl (which contains chloride ions) plays an essential part in expediting the ion transfer process, which gives a high potential reading and, subsequently, a rapid recovery time [25].

Figure 9 shows similar results for PIM and Neosepta AM-01 membrane and much worse results for the CTA membrane. The highest Pd^{2+} ions recovery after 30 min was achieved by PIM (99.9 %), followed by Neosepta AM-01 membrane (96.0 %). In contrast, a pure CTA membrane used as an ion exchange membrane could not fully recover Pd^{2+} ions, even after 240 minutes, when only up to 60 % of Pd^{2+} ions are recovered. This result proves that using hybrid PIM consisting of silane can increase the recovery rate of Pd^{2+} ions. Moreover, the presence of ionic liquid (BMIM-Cl) led to this result. The ionic liquid's role is to facilitate the movement of the ions across the membrane due to the presence of Cl^- ions [23]. Additionally, silane provides additional strength to PIM, where the hydrated micro channels are formed from the mixture of hydrophilic and charged groups. These microchannels become the passage for the ions to transfer across the membrane [29].

The prepared PIM and Neosepta AM-01 membrane reusability study was also conducted (60 min of recovery time). After five cycles of recovery test, it was found that PIM could maintain the

recovery performance with only 4 % of decreased performance while Neosepta AM-01 membrane has lost up to 8 % of recovery performance. These results also confirmed the suitability of PIM to be used as an anion exchange membrane.

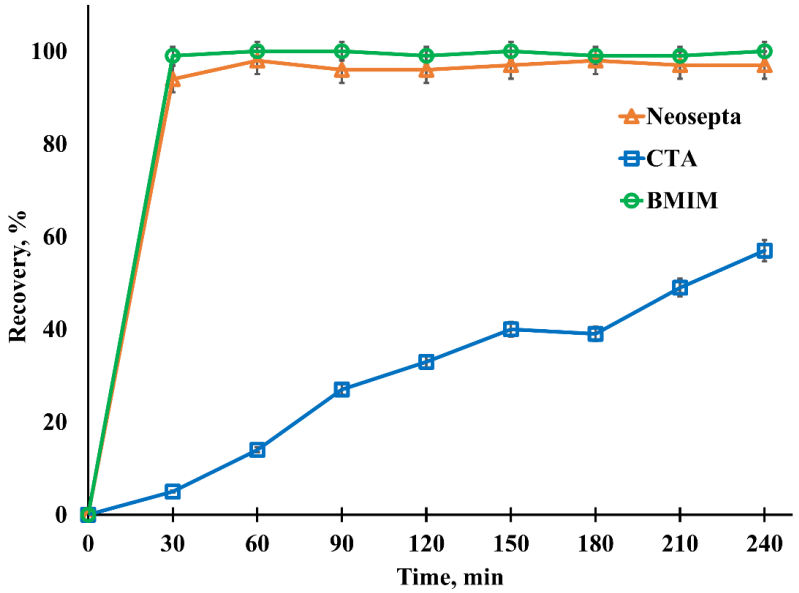

***Figure 9**. Influence of different types of the membrane towards the recovery of 100 mg/L of Pd^{2+} in 0.2 M NaCl*

Polarization study

A polarization study was conducted to investigate the deviation of the electrochemical process from equilibrium due to the passing of electric current through the electrogenerative reactor. It can be seen in Figure 10, different types of anion exchange membranes produce current densities of 5.3 mA cm^{-2} (Neosepta AM-01 membrane) and 4.6 mA cm^{-2} (hybrid PIM) in the short-circuited condition when voltage is 0.0 V. It is desirable to have high current densities in the electrogenerative process because it will provide faster kinetics for the deposition process [23]. The RVC shows less polarization in the range of 0 to 0.45 mA cm^{-2} for both membranes (hybrid PIM and Neosepta AM-01 membrane), which suggests a great flow of electrons between the cathode (RVC) and anode (zinc foil). These results show that the polarization performance of the hybrid PIM used in this study is on par with the commercially available membrane.

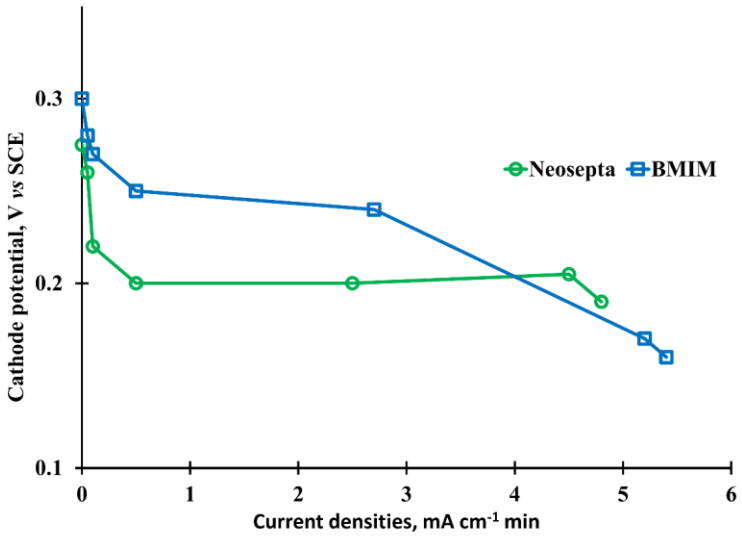

***Figure 10.** Polarization curves of RVC cathode using different types of ion exchange membrane*

The kinetic study of the mass-controlled process for different types of membranes was also performed. Based on Figure 11, the concentration [C_t/C0] decreased as the time increased. Moreover, it was noticed that the concentration of Pd^{2+} ions decreased from initial values to less than 0.1 mg/L after 30 min with the hybrid PIM used as the anion exchange membrane. This shows that hybrid PIM is the most suitable anion exchange membrane for recovering Pd^{2+} ions in this study.

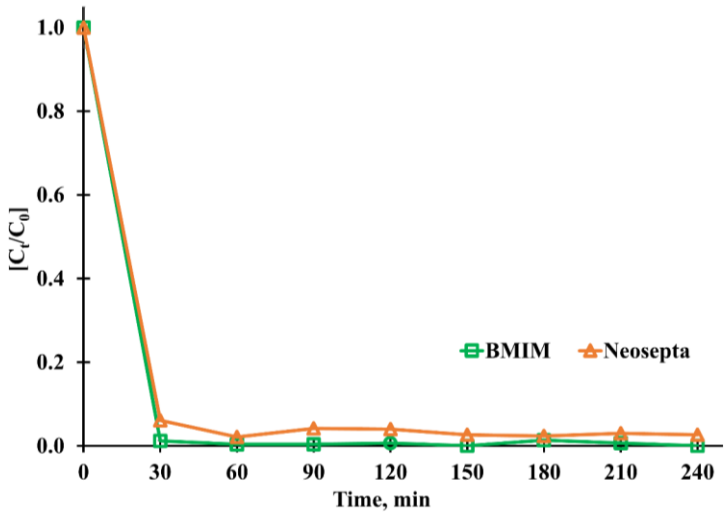

Figure 11. *Normalized concentration [Ct/C_0] vs time between hybrid PIM and commercial membrane Neosepta for deposition of 100 mg/L of Pd^{2+} in 0.2 M NaCl*

Conclusions

In this study, a series of hybrid PIM membranes containing CTA, silane mixture and different ionic liquids has been successfully prepared and used as an anion exchange membrane in the electrogenerative process of Pd ions. The electrogenerative process showed that hybrid PIM made up of CTA, BMIM-Cl and silane mixture with respective compositions of 0.10, 0.08 and 0.03 g, performs well as an anion exchange membrane. Furthermore, compared to a commercially available anion exchange membrane, this hybrid PIM achieves a full percentage recovery of Pd^{2+} ions in a shorter time (30 min). Thus, hybrid membranes can potentially replace expensive commercially available anion exchange membranes.

Acknowledgements: *The authors would like to thank Nippon Sheet Glass Foundation for Materials Science and Engineering, Japan (304 / PKIMIA / 6501008) for funding this research.*

References

[1] J. Kanagaratnam, F. B. M. Suah, An innovative use of electrochemically modified three-dimensional carbon felt for a rapid recovery of gold from diluted chloride solution, *Journal of Chemical Technology & Biotechnology* **96(8)** (2021) 2219-2227. https://doi.org/10.1002/jctb.6736

[2] M. N. Jajuli, N. Mohamed, F. B. M. Suah, Electrochemical removal of cadmium from a sulphate solution using a three-dimensional electrode, *Alexandria Engineering Journal* **59(6)** (2020) 4237-4245. https://doi.org/10.1016/j.aej.2020.07.027

[3] N. A. Roslan, F. B. M. Suah, N. Mohamed, Influence of different 3-D electrodes towards the performance of gold recovery by using an electrogenerative process, *Arabian Journal of Chemistry* **13(1)** (2020) 1440-1448. https://doi.org/10.1016/j.arabjc.2017.11.015

[4] F. B. M. Suah, B.P . Teh, N. Mansor, H. H. Hamzah, N. Mohamed, A closed-loop electrogenerative recycling process for recovery of silver from a diluted cyanide solution, *RSC Advances* **9(54)** (2019) 31753-31757. https://doi.org/10.1039/C9RA05557F

[5] S. Jiang, H. Sun, H. Wang, B. P. Ladewig, Z. Yao, A comprehensive review on the synthesis and applications of ion exchange membranes, *Chemosphere* **282** (2021) 130817. https://doi.org/10.1016/j.chemosphere.2021.130817

[6] R. Pärnamäe, S. Mareev, V. Nikonenko, S. Melnikov, N. Sheldeshov, V. Zabolotskii, H.V.M. Hamelers, M. Tedesco, Bipolar membranes: A review on principles, latest developments, and applications, *Journal of Membrane Science* **617** (2021) 118538. https://doi.org/10.1016/j.memsci.2020.118538

[7] W. You, K. J. T. Noonan, G. W. Coates, Alkaline-stable anion exchange membranes: A review of synthetic approaches, *Progress in Polymer Science* **100** (2020) 101177. https://doi.org/10.1016/j.progpolymsci.2019.101177

[8] A. Breytus, Y. Huang, D. Hasson, R. Semiat, H. Shemer, A comparative study on Donnan dialysis separation using homogeneous and heterogeneous anion-exchange membranes, *Desalination and Water Treatment* **225** (2021) 1-10. https://doi.org/10.5004/dwt.2021.27305

[9] J.-M.A. Juve, F.M.S. Christensen, Y. Wang, Z. Wei, Electrodialysis for metal removal and recovery: A review, *Chemical Engineering Journal* **435(2)** (2022) 134857. https://doi.org/10.1016/j.cej.2022.134857

[10] J. Lei, X. Liu, X. Chen, H. Luo, W. Feng, J. Zhang, F. Liu, S. Pei, Y. Zhang, Ultra-bubble-repellent sodium perfluorosulfonic acid membrane with a mussel-inspired intermediate layer for high-efficiency chlor-alkali electrolysis, *Journal of Membrane Science* **644** (2022) 120181. https://doi.org/10.1016/j.memsci.2021.120181

[11] L. Liu, Y. Lu, C. Ning, N. Li, S. Chen, Z. Hu, Comb-shaped sulfonated poly (aryl ether sulfone) proton exchange membrane for fuel cell applications, *International Journal of Hydrogen Energy* **47(36)** (2022)16249-16261. https://doi.org/10.1016/j.ijhydene.2022.03.134

[12] Y. Liu, J. Ding, H. Zhu, X. Wu, L. Dai, R. Chen, B. Van der Bruggen, Recovery of trivalent and hexavalent chromium from chromium slag using a bipolar membrane system combined with oxidation, *Journal of Colloid and Interface Science* **619** (2022) 280-288. https://doi.org/10.1016/j.jcis.2022.03.140

[13] J. Ran, L. Wu, Y. He, Z. Yang, Y. Wang, C. Jiang, L. Ge, E. Bakangura, T. Xu, Ion exchange membranes: New developments and applications, *Journal of Membrane Science* **522** (2017) 267-291. https://doi.org/10.1016/j.memsci.2016.09.033

[14] B. Swanckaert, J. Geltmeyer, K. Rabaey, K. De Buysser, L. Bonin, K. De Clerck, A review on ion-exchange nanofiber membranes: properties, structure and application in electrochemical (waste)water treatment, *Separation and Purification Technology* **287** (2022) 120529. https://doi.org/10.1016/j.seppur.2022.120529

[15] D. Tichý, Z. Slouka, Semi-Continuous Desalination and Concentration of Small-Volume Samples, *International Journal of Molecular Sciences* **22(23)** (2021) 12904. https://doi.org/10.3390/ijms222312904

[16] K. Xu, S. Pei, W. Zhang, Z. Han, G. Liu, X. Xu, J. Ma, Y. Zhang, F. Liu, Y. Zhang, L. Wang, Y. Zou, H. Ding, P. Guan, Chemical stability of proton exchange membranes synergistically promoted by organic antioxidant and inorganic radical scavengers, *Journal of Membrane Science* **655** (2022) 120594. https://doi.org/10.1016/j.memsci.2022.120594

[17] W. W. Guan, X. Y. Shi, T. T. Xu, K. Wan, B. W. Zhang, W. Liu, H. L. Su, Z. Q. Sou, Y. W. Du, Synthesis of well-insulated Fe–Si–Al soft magnetic composites via a silane-assisted organic/inorganic composite coating route, *Journal of Physics and Chemistry of Solids* **150** (2021) 109841. https://doi.org/10.1016/j.jpcs.2020.109841

[18] Y. Mo, L. Zhang, X. Zhao, J. Li, L. Wang, A critical review on classifications, characteristics, and applications of electrically conductive membranes for toxic pollutant removal from water: Comparison between composite and inorganic electrically conductive membranes, *Journal of Hazardous Materials* **436** (2022) 129162. https://doi.org/10.1016/j.jhazmat.2022.129162

[19] I. Paulraj, V. Lourdhusamy, C.-Y. Liu, Organic/Inorganic n-type PVDF/$Cu_{0.6}Ni_{0.4}$ hybrid composites for thermoelectric application: A thermoelectric generator made of 8 pairs of p-leg ZnSb/Sb and n-leg β-PVDF/$Cu_{0.6}Ni_{0.4}$, *Chemical Engineering Journal* **446** (Part 3) (2022) 137083. https://doi.org/10.1016/j.cej.2022.137083

[20] S. S. Todkar, S. A. Patil, Review on mechanical properties evaluation of pineapple leaf fibre (PALF) reinforced polymer composites, *Composites Part B: Engineering* **174** (2019) 106927. https://doi.org/10.1016/j.compositesb.2019.106927

[21] D. R. Dekel, Review of cell performance in anion exchange membrane fuel cells, *Journal of Power Sources* **375** (2018) 158-169. https://doi.org/10.1016/j.jpowsour.2017.07.117

[22] P. Xu, Y. Luo, P. Zhang, Interfacial architecting of organic–inorganic hybrid toward mechanically reinforced, fire-resistant and smoke-suppressed polyurethane composites, *Journal of Colloid and Interface Science* **621** (2022) 385-397. https://doi.org/10.1016/j.jcis.2022.04.082

[23] N. Mansor, N. Mohamed, F. B. M. Suah, Electrochemical recovery of low concentration of palladium from palladium (II) chloride of electroplating wastewater, *Journal of Chemical Technology & Biotechnology* **96(11)** (2021) 3216-3223. https://doi.org/10.1002/jctb.6878

[24] N. A. Roslan, F. B. M. Suah, N. Mohamed, The use of an electrogenerative process as a greener method for recovery of gold (III) from the E-waste, *Separation and Purification Technology* **182** (2017) 1-8. https://doi.org/10.1016/j.seppur.2017.03.032

[25] F. B. M. Suah, N. A. Roslan, N. F. Dahlan, N. Mohamed, A use of polymer inclusion membrane as anion exchange membrane for recovery of Cu(II) ions based on an electrogenerative system, *Journal of The Electrochemical Society* **165(7)** (2018) H310. https://doi.org/10.1149/2.0101807jes

[26] N. Mansor, N. Mohamed, F. S. Mehamod, F. B. M. Suah, Galvanic deposition of Pd^{2+} ion in chloride solution by using different three dimensional electrodes, *Journal of Electroanalytical Chemistry* **838** (2019) 23-32. https://doi.org/10.1016/j.jelechem.2019.02.014

[27] M. Resina, J. Macanás, J. De Gyves, M. Muñoz, Zn (II), Cd (II) and Cu (II) separation through organic–inorganic hybrid membranes containing di-(2-ethylhexyl) phosphoric acid or di-(2-ethylhexyl) dithiophosphoric acid as a carrier, *Journal of Membrane Science* **268(1)** (2006) 57-64. https://doi.org/10.1016/j.memsci.2005.06.008

[28] M. Resina, J. Macanás, J. De Gyves, M. Muñoz, Development and characterization of hybrid membranes based on an organic matrix modified with silanes for metal separation, *Journal of Membrane Science* **289(1-2)** (2007) 150-158. https://doi.org/10.1016/j.memsci.2006.11.049

[29] F. Hu, H. Hu, J. Tang, X. Qiu, W. Jin, J. Hu, Plasticization-induced oriented micro-channels within polymer inclusion membranes for facilitating Cu (II) transport, *Journal of Molecular Liquids* **301** (2020) 112457. https://doi.org/10.1016/j.molliq.2020.112457